

Residual In-plane Mechanical Properties of Transversely Crushed Structural Foams

VITALY KOISSIN*

Department of Metallurgy and Materials Engineering, Katholieke Universiteit Leuven, Kasteelpark Arenberg 44, B-3001 Leuven, Belgium

ANDREY SHIPSHA†

Department of Aeronautical and Vehicle Engineering, Royal Institute of Technology, Teknikringen 8, S100 44 Stockholm, Sweden

ABSTRACT: The mechanical properties of structural polymer foams are investigated after crushing in the rise direction (out-of-plane axis of a foam material block). The crushed foams are loaded in uniaxial compression, tension, or shear. All tests are performed in the plane of the foam block, i.e., perpendicular to the crushing direction. For comparison, virgin foams are also characterized. The results are discussed featuring the properties of crushed foams, which can be important for the damage tolerance analysis of a foam core sandwich structure.

KEY WORDS: sandwich structure, crushed foam core, mechanical properties.

INTRODUCTION

IN A FOAM core sandwich structure, by virtue of low bending stiffness of thin faces and low strength of a lightweight core, the latter can undergo a local crushing. Therefore, the properties of the crushed foam should be determined and accounted for in the accurate damage tolerance analysis. For instance, the crushed foam core underlying an impact damage can impose a crack onset and failure under overall bending of the sandwich beam [1].

Previous studies [2–4] have shown a drastic decrease of the foam stiffness in the direction of previous crushing. The mechanical properties in the direction perpendicular to the crushing received less attention [5,6].

*Author to whom the correspondence should be addressed. Email: vitaly@kth.se

†Present address: Inspecta Sverige, Warfvinges väg 19B, S-104 25 Stockholm, Sweden.
Figures 1–8 appear in color online: <http://jasm.sagepub.com>

In the present study, the stress–strain behavior of several pre-crushed (up to the densification onset) polymeric foam materials is characterized under uniaxial compression, tension, or shear. The test direction is perpendicular to the crush direction. The tests are conducted at ambient temperature and humidity. The experimental results are compared with the test data for virgin foam materials.

VIRGIN FOAM CRUSHING

Five rigid cellular foams are considered; Rohacell WF51 and Divinycell H60, H100, H130, and H200. These foams are produced by expansion of liquid components in a mould and typically used as cores in sandwich structures for marine (Divinycell H-grade) or low-performance aerospace (Rohacell WF-grade) applications. All foams have a closed-cell structure and nominal densities of 51, 60, 100, 130, and 200 kg/m³, respectively [7,8].

Crushing of foams is performed on prismatic pieces cut from the foam material block. The height of the piece, h_c , is equal to the thickness of the supplied foam blocks (50 mm for all the foams). The piece is crushed under uniform compressive load, applied in the thickness direction by two parallel rigid plates. The loading is performed under displacement control at 2 mm/min until the densification onset as schematically shown in Figure 1(left). Path A–B corresponds to the elastic response. Then, the tested foam materials exhibit inelastic compressibility (crushing) due to bending and buckling of cell walls leading to their collapse. As a result, the response curve has a long crushing plateau, path B–C. When the cells are almost completely compacted, i.e., the local compressive strain reaches the densification strain ($\varepsilon_d = 68\%$ for WF51, 48–51% for other tested foams),

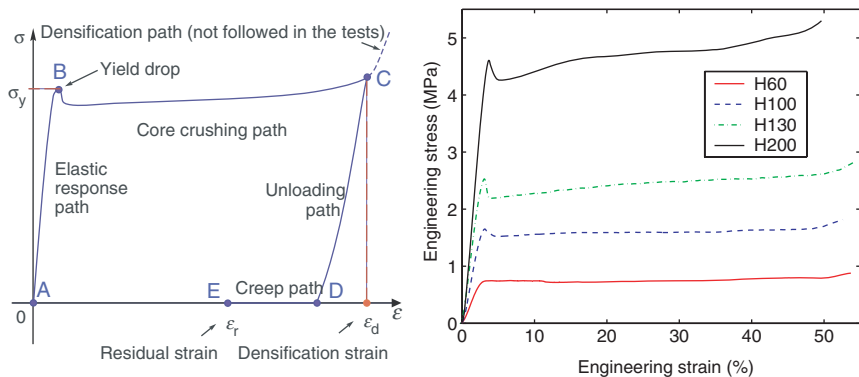


Figure 1. Schematic of the load history (left) and the real view of the stress–strain curves (right, unloading path is not shown) under uniaxial compression.

the stress increases quickly. In the present study, the densification path is not followed, and the specimens are unloaded after reaching point C.

More detailed description of densification tests is provided by the authors in [4]. Typical stress–strain curves are presented in Figure 1 (right) for H-grade foams (only loading path is shown). It can be seen that the densification strain is slightly dependent on the density of H-grade foams (Table 1). This fact disagrees with the published experimental data for some other foam materials [9].

The crushed foams exhibit a significant strain creep, path D–E, within first 30 s after unloading [4]. In order to reach an ‘equilibrium’ state of a crushed foam material, the crushed piece is held in free state during several hours. The average values of residual strain, ε_R , and measured densities are listed in Table 1. It is interesting to note that this value for 50 mm thick H130 foam (44%) exceeds the one for 40 mm thick H130 foam ($\approx 15\%$, [4]) about in 2 times. This discrepancy is believed to be due to a difference in production for these two foam blocks.

X-RAY PROJECTION

It is known that the mechanical properties are strongly dependent on the density of a cellular material [9]. In order to investigate the density variation through the thickness of a foam block, the X-ray analysis is performed for WF51, H60, and H200 materials. The images are taken using AEA Tomohawk system with the resolution 66.1 $\mu\text{m}/\text{pixel}$, voltage 60 kV, and current 0.58 mA. The depth of the specimens is 55 mm; no filter is used. A gray-scale picture is analyzed by the Matlab applet, where the relative through-the-thickness density distribution is calculated for each pixel column and then averaged on the specimen width (also 55 mm). Only a minor (<3%) variation is detected both for the virgin and crushed WF51 foam, Figure 2 (left). The same is seen for the virgin H60 material, Figure 2 (middle), while the crushed one shows a distinct density drop of $\sim 13\%$ nearby the free surfaces. For H200 foam, a prominent ($\pm 10\%$)

Table 1. Out-of-plane compression test results (virgin foam/transversally pre-crushed foam).

Foam (50 mm thick):	WF51	H60	H100	H130	H200
Densification strain ε_d (%)	68	50	48	51	46
Residual strain* ε_R (%)	51	27	17	32	30
Density ** (kg/m ³)	56/115	62/81	95/109	124/173	194/257

*Measured several hours later the pre-crushing, **The crushed foam density is calculated accounting for a small growth of the cross-sectional area.

nonuniformity is seen in the virgin state, Figure 2 (right); contrary to H60, this becomes milder after the crushing.

For H200, it is interesting to note that the density has the minimum not only at the middle of the thickness but also close to the surfaces of the foam material block. Similar sinusoidal density distribution is reported in study [10]; however, a single minimum (no drop at the surface) is observed, similar to the present data for WF51. In Ref. [11], an opposite result is mentioned with a single maximum at the middle of the thickness. Figure 2 (right) shows that the density variation decreases after the foam crushing. The shape of the distribution changes also, especially at the middle of the specimen, where the lowest density is obtained for the virgin H60 and H200 materials. This fact indicates that the densification and residual strains are nonuniform through the thickness of the crushed foam specimens.

An indirect evidence of the density distribution follows from the densification test, section ‘Virgin foam crushing’. There, the crushing of H-grade foams always initiates nearby the middle of the thickness and then spreads sideways. The most of the WF51 specimens start to crush at the lower and/or upper surface; then, compaction spreads gradually toward the midplane. The latter observation is probably due to a negligibly small density variation in this foam material, Figure 2 (left).

IN-PLANE TESTING OF VIRGIN AND CRUSHED FOAM

Compressive Properties

The in-plane compression is performed using a cylindrical specimen bonded between aluminum cylinders, which are rigidly fit in the testing machine. The length of the specimen is 50 mm in all cases. For the virgin foam specimens, the diameter is equal to the thickness, h_c , of the foam material blocks that is also 50 mm. The pre-crushed foam specimens have different

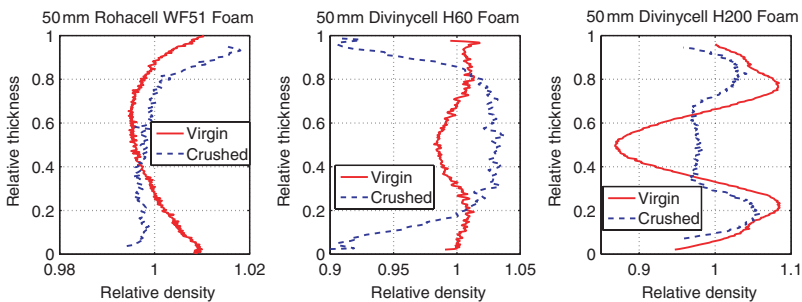


Figure 2. Through-the-thickness density distribution for WF51 (left), H60 (middle), and H200 (right) foams.

diameters depending on the thickness, $h_c(1 - \varepsilon_R)$, of a crushed foam material block. The specimens are compressed up to 0.4% of strain at the displacement rate of 2 mm/min; the strain is measured using an extensometer. Measured Young's moduli are given in Table 2. Taking the scatter into account, the difference between virgin and pre-crushed foams is not significant, with the exception of H130 material. A comparison of in-plane Young's moduli for crushed foams with relevant data for the out-of-plane direction, [4], reveals that crushing leads to prominent orthotropy of the properties.

Tensile properties

The in-plane tension is performed for two types of specimens; 1) cylindrical (only H-grade foams) or 2) thin 'dog-bone' shaped. The former set-up is the same as in the compression tests described above; the same samples are used after the small-strain compression. The only difference is that the loading fixture is self-aligning in tension in order to avoid an eccentric load as much as possible, Figure 3 (left). The specimens are loaded with a constant rate of 2 mm/min. Since no waist is machined, the failure is observed at the epoxy adhesive layer between the foam and an aluminum cylinder. Data in Table 3 show that the mechanical properties, in general, increase after crushing. One exception is the Young's modulus of H60 foam. It can be suggested that a weakening of its cell structure after crushing is not compensated by an increased density, due to a relatively low residual strain ($\varepsilon_R=27\%$). If compare with Table 2, it is also seen that both test methods (compression and tension) yield close results for the Young's modulus; the maximal difference in 19% appears for the crushed H60 foam ($54.1/45.6 \approx 1.19$).

Alternative tensile tests are processed according to ASTM D638 (Test Method for Tensile Properties of Plastics). The $150 \times 25 \times 9$ mm specimens are sliced from the inner or outer layers of a foam material block. The exception is the pre-crushed WF51 block, which is cut at the midplane only into two layers due to its small thickness (24.3 mm). In order to ensure that the fracture occurs within 50 mm gauge length of the extensometer, the central 80 mm long part of the slices is machined like a 'dog-bone' to the same 50 mm length with 10×9 mm cross-section, Figure 3 (right).

Table 2. In-plane compression test results (virgin foam/transversally pre-crushed foam).

Foam (50 mm thick):	WF51	H60	H100	H130	H200
Young's modulus, MPa:	66.1/68.9	48.0/54.1	87.5/92.7	112.6/183.2	232.6/256.3

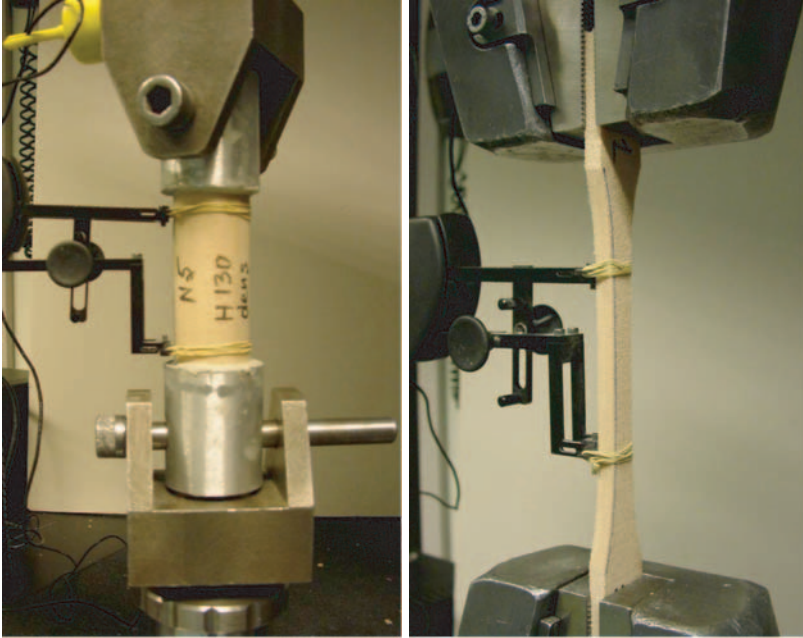


Figure 3. Tensile tests on pre-crushed H130 (left) and virgin H100 (right) foams.

Table 3. In-plane tension test results (virgin foam/transversally pre-crushed foam).

Foam	Specimen	Layer	Young's modulus (MPa)	Ult. stress (MPa)	Ult strain (%)
WF51	'Dog-bone'	Outer	85.4/71.6 ^a	1.65/1.55 ^a	2.7/5.3 ^a
	'Dog-bone'	Inner	79.1/71.6 ^a	1.51/1.55 ^a	2.5/5.3 ^a
H60	Cylindrical	–	59.1/45.6	0.98/1.20	1.8/4.2
	'Dog-bone'	Outer	51.2/47.5	1.31/1.58	4.2/5.7
	'Dog-bone'	Inner	47.5/34.4	1.23/1.23	6.5/7.5
H100	Cylindrical	–	85.2/100.5	2.42/2.85	3.6/5.8
	'Dog-bone'	Outer	89.5/111.4	2.54/3.26	4.9/6.7
	'Dog-bone'	Inner	84.8/82.4	2.48/2.51	5.5/7.7
H130	Cylindrical	–	116.6/163.2	2.60/3.95	2.6/4.4
	'Dog-bone'	Outer	135.7/171.0	3.65/5.09	6.1/9.2
	'Dog-bone'	Inner	96.8/127.5	2.84/3.92	7.3/8.7
H200	Cylindrical	–	205.4/243.5	2.84/4.60	1.5/2.6
	'Dog-bone'	Outer	210.6/265.9	5.74/7.81	8.8/12.4
	'Dog-bone'	Inner	171.6/231.8	4.82/7.21	12.3/14.0

^aAveraged between the Outer and Inner layers.

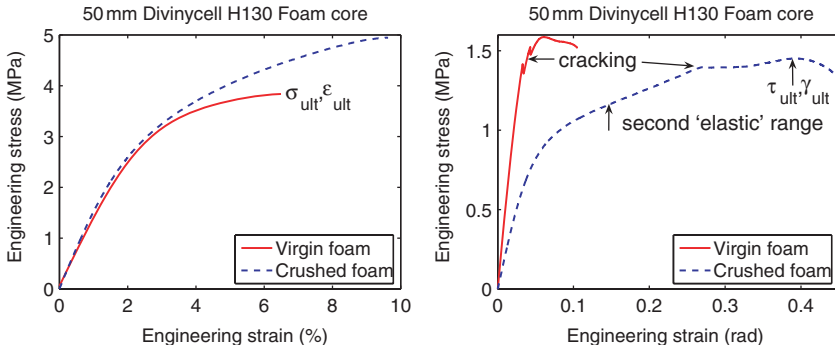


Figure 4. Typical response curves under tension on outer layer 'dog-bone' specimens (left) and shearing on prismatic specimens (right), H130 foam.

The specimens are loaded in the displacement rate of 2 mm/min. Typical stress-strain curves sampled from these tests are shown in Figure 4 (left). The averaged test results are given in Table 3. It can be seen that the in-plane Young's modulus for pre-crushed foams is typically higher (35% for H200 foam) in comparison with the data for virgin foams. The same trend is observed for the tensile strength at break of the outer layers; the maximal rise consists 39% (H130). As for the inner layers, their strength is either almost equal in the virgin and pre-crushed states (WF51, H60, and H100) or also increases after the crushing in a proportion similar to that of the outer layers (H130 and H200). The elongation at break of the pre-crushed foams always higher than that of the virgin foams, e.g., by the factor of 2 for WF51 foam. It can also be derived from Table 3 that the pre-crushing increases (mostly for H60 and H100) or decreases (mostly for H130 and H200) the difference between the mechanical properties of the outer and inner layers; this change can be rather considerable.

If compare the tests on cylindrical and 'dog-bone' specimens, it is usually seen that the former give lower ultimate values. This is due to the constant cross-section provoking to a stress concentration and premature failure at the bond line with the fixture. Sometimes, the cylindrical specimens give higher results than the 'dog-bone' specimens. This is probably because of the fact that a smaller cross-section includes more (in percentage terms) damaged surface cells and thus can be more weakened in stiffness and strength. It is also worth to note that the thickness of the pre-crushed 'dog-bone' specimens increases by 5–10% under the tension (negative Poisson's ratio) obviously due to unbending of the cell walls and other micro-mechanical features. The real ultimate stresses are, therefore, slightly lower than given in Table 3.

Shear Properties

The shear tests are performed according to ASTM C273 (Standard Test Method for Shear Properties of Sandwich Core Materials). A brick specimen with in-plane dimension 300×75 and the thickness of $h_c(1 - \varepsilon_R)$ mm, Table 1, is bonded between two rigid parallel loading plates and subjected to shearing with the load line passing close the specimen diagonal, Figure 5. The constant cross-head speed of 3 mm/min is used. The shear angle (averaged over the thickness) is calculated through a relative displacement of the loading plates; this sliding is measured using an extensometer placed between two magnetic holders attached to each plate. Typical shear responses are plotted in Figure 4 (right). It is seen that the linear behavior is observed first; then, the slope decreases with increasing load. The pre-crushed H-grade foams have also a second region of the linear response at large strains; the corresponding slope is denoted in Table 4 as the 'secant modulus'. No such effect is observed for the pre-crushed WF51

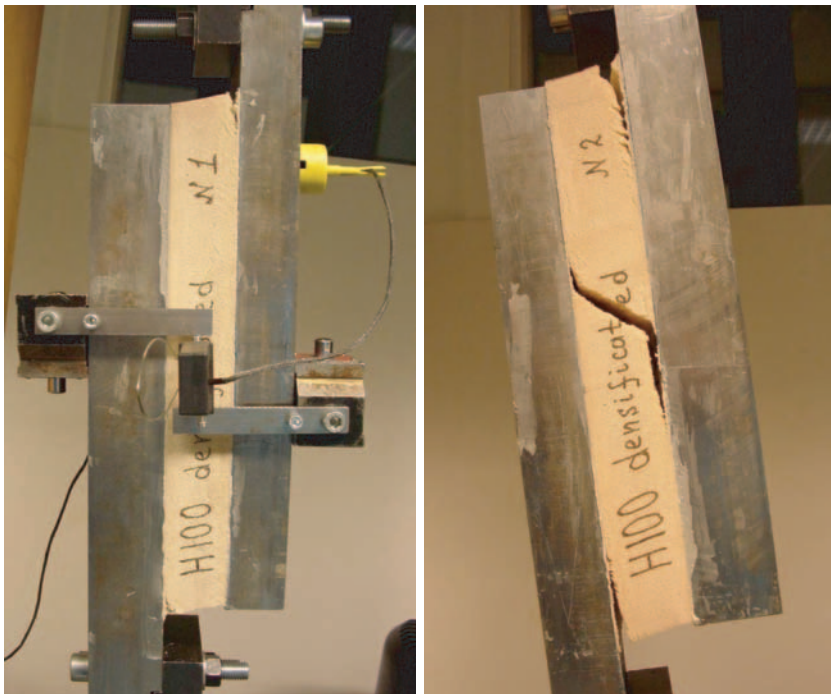


Figure 5. Typical shear test on pre-crushed H100 foam; crack onset in the bottom left and upper right corners (left) and final failure (right).

foam; for it, the slope of the load curve decreases monotonically along with the shear strain.

Slips in the final part of the curves are caused by cracks at the diagonally opposite corners of a foam brick, Figure 5 (left). Upon formation of these cracks, the specimen continues to resist the applied load but with a reduced shear stiffness. The governing failure modes are either an abrupt shearing along the specimens's midplane (WF51 foam) or complete debonding of a loading plate due to an unstable growth of a corner crack (H-grade foams). For the pre-crushed H100, H130, and H200 foams, a 45° shear crack occurs also at the specimen middle prior to the gross failure, Figure 5 (right).

The test results are summarized in Table 4. For the virgin foams, the magnitudes of the shear moduli agree well with the ones estimated through the average Young's modulus in tension (Table 3, 'dog-bone' specimens); the maximal difference does not exceed 13%. The pre-crushed foams show lower shear stiffness (by a factor 1.5–5), 10–50% lower ultimate stress, and higher deformability (by a factor 3–5) if compare with the virgin foams. However, the ultimate values should be treated as approximate, since the real stress–strain state differs from the pure shear even at small strains due to the free edges effect. A nonstandard ratio between the specimen length and thickness can also alter the tests results. This is since C273 method dictates that this aspect ratio should not be less than 10, while it is between 5 (all virgin foams) and 12 (crushed WF51 foam) in the present study. However, it is known that the prescribed minimal ratio does not necessarily result in the most accurate measurement, [13]. Another, probably principal, source of discrepancy is the cracks causing change of the test configuration and premature final failure. Under increasing load, the cracks propagate along the bonding lines. As a result, the load is carried by a smaller area than used in calculations through the initial specimen length. Finally, the specimen thickness is also changed somehow at large shear angles, especially when testing a crushed foam material.

Table 4. In-plane shear test results (virgin foam/transversally pre-crushed foam).

Foam	Shear modulus (MPa)	Secant modulus ^a (MPa)	Ult. stress (MPa)	Ult. strain (grad)
WF51	26.0/5.2	–/–	0.52/0.24	1.2/4.6
H60	18.3/6.9	–/1.8	0.54/0.46	2.9/12.6
H100	35.2/15.0	–/2.6	1.23/0.97	4.0/15.5
H130	50.7/20.6	–/1.9	1.59/1.44	4.0/21.8
H200	64.4 ^b /41.8	–/2.6	2.90 ^b /2.75	9.7 ^b /26.4

^aSecant shear modulus within the second elastic range, see Figure 4 (right).

^bTaken from [12].

FINITE-ELEMENT ANALYSIS OF THE SHEAR TEST

The finite element (FE) analysis of C273 shear test is performed to quantify the sensitivity of the shear stiffness to through-the-thickness density variation. Study [11] reported minor changes ($<1\%$) in linear shear stiffness at the density variation of 10%, in the case of a single minimum at the middle of a foam thickness. In the present study, an FE problem is considered to model the shear behavior of the virgin H200 with 3 density minimums, Figure 2 (right). The specimen is meshed as 2D rectangular domain using 4-node isotropic shell elements. The loading plates are meshed using rigid bar elements. Schematic of the FE model is shown in Figure 6 (left).

Two cases are studied in the FE analysis; (1) even and (2) uneven stiffness distribution through the thickness. In the latter case, the foam domain is subdivided into 25 layers; each layer is associated with certain Young's modulus as shown in Figure 6 (right). Sinusoidal distribution is accepted according to the detected density variation shape, Figure 2 (right). The maximum (210.6 MPa) and minimum (171.6 MPa) values are taken from Table 3, thus approximately representing the outer and inner layers of the real material. In the 'even' model, constant Young's modulus of 195.2 MPa is used;

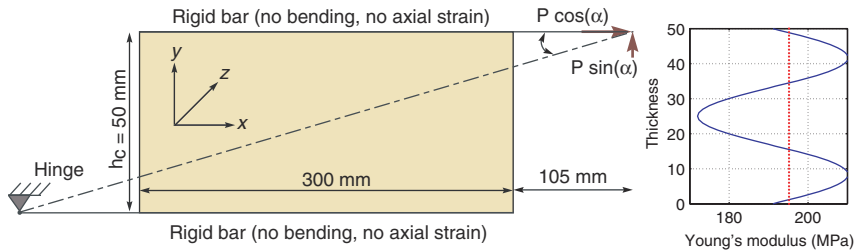


Figure 6. Schematic of the FE model (left, undeformed, not drawn to scale) and applied distribution of the Young's modulus (right).

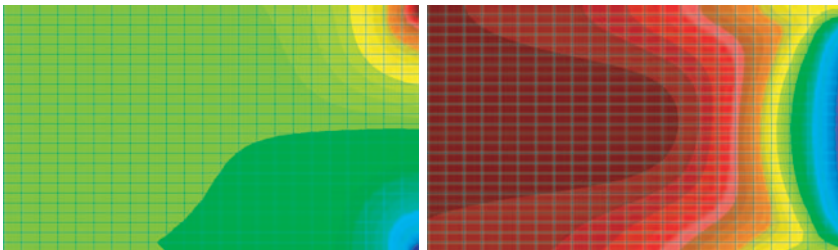


Figure 7. Details of the normal σ_y (left) and shear (right) stress fields in the FE model. Uneven stiffness distribution.

this is the average value of the uneven distribution function. The Poisson's ratio of 0.32 is applied in both models, following the manufacturer's data sheet [8].

The linear-elastic analysis shows that the shear stress (τ_{xy}) fields are similar in both cases. The stress concentration is dominated by the tension/compression (σ_y) at the specimen corners. The overall shear modulus stays almost the same, although the 'uneven' model is more compliant (70.3 MPa vs. 72.5 MPa, 3% difference). Comparison of the former value with the experimental one, Table 4, gives the difference in 9%. The latter value is in a good agreement with the theoretical estimation $195.2/2(1 + 0.32) = 73.9$ MPa.

DISCUSSION AND CONCLUSIONS

Experimental characterization of pre-crushed structural foams was performed in this study. The main results can be outlined as

- Significant through-the-thickness nonuniformity of the density distribution is measured for Divinycell H200 foam. After pre-crushing, the shape of the distribution changes; this indicates that the residual strains are nonuniform through the thickness of the crushed foam specimen. Similar effect is observed for crushed H60 material;
- Variations in local density lead to a prominent variability of the in-plane Young's modulus in different layers of the foam material block. The pre-crushing can increase/decrease this difference in several times. For the overall shear modulus, the influence of the local density ($\pm 10\%$) is negligibly small;
- Except for Divinycell H130 foam material, the in-plane compression Young's modulus stays almost the same after the crushing, despite of a highly increased overall density. This fact should be attributed to a very compliant compression behavior of the crushed foam cells;
- Under in-plane tension, the crushed foam materials exhibit usually improved mechanical properties. However, this is not always the case if considering the effective (related to the actual density) values. Figure 8 shows the relative drop in the specific stiffness and strength properties. The plots reveal that the crushing produces usually a detrimental effect, especially under the shear. The exception is tension of H100, H130, and H200 foams, which preserve the specific stiffness and even slightly increase the specific strength after being crushed. The ultimate strain always rises after the pre-crushing, Tables 3 and 4 again, this is most prominent for the shear tests.

The results of this study may contribute to the damage tolerance analysis of sandwich structures having a zone of a crushed foam core. However, it should be pointed out that the presented tests data are related only to the

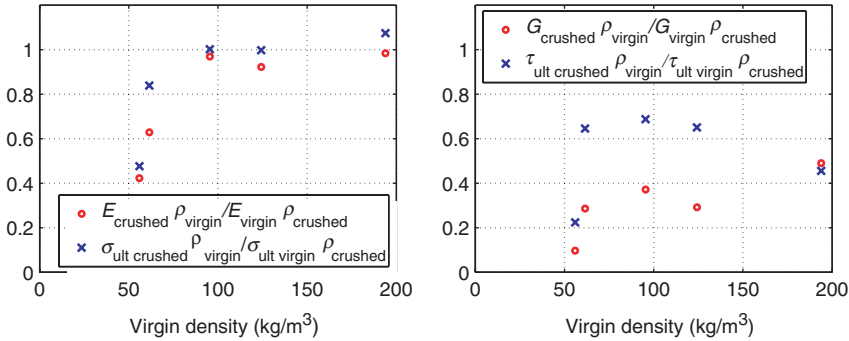


Figure 8. Relative change in the stiffness and strength after pre-crushing, under uniaxial tension (left, 'dog-bone' specimens) and shear (right).

case of a single pre-crushing and relaxed state of the crushed material, Figure 1(left). This is of course not a common case for real sandwich structures, where the crushed foam core undergoes a more complex residual stress-strain state. For the Young's and shear moduli, one can roughly suggest that the present test data for $\sigma_E=0$ (stress corresponding to point E in Figure 1(left)) can be scaled for the case of arbitrary σ_E in the same proportion as the density changes; the ultimate values require a particular experimental study. The influence should also be investigated of the multiple out-of-plane compression-tension on a possible degradation of the in-plane mechanical properties. Furthermore, the test results may depend on the production conditions of a particular core panel, heat/light aging, strain rate, temperature, humidity conditions, etc. The presented data should thus be considered as approximate even within the used test methods.

ACKNOWLEDGMENTS

The authors are thankful to Prof. Dan Zenkert (Royal Institute of Technology, Stockholm, Sweden), Prof. Vitaly Skvortsov (State Marine Technical University, St-Petersburg, Russia), and Prof. Stepan Lomov (Katholieke Universiteit Leuven, Belgium) for their interest to this study and valuable comments. Ms Greet Kerckhofs and Mr Dmitry Ivanov (ibid) are gratefully acknowledged for the help with X-ray and full-field strain measurements. Authors would also like to thank Mr Kris Van de Staey (ibid) and Mr Anders Beckman (laboratory of the Dept of Aeronautics, Royal Institute of Technology) for assistance with the mechanical testing. Thank also to Röhm GmbH and Divinycell International AB for supplying the foam materials.

REFERENCES

1. Shipsha, A., Hallström, S. and Zenkert, D. (2003). Failure Mechanisms and Modelling of Impact Damage in Sandwich Beams—A 2D Approach: Part I—Experimental Investigation, *Journal Sandwich Structures and Materials*, **5**(1): 7–32.
2. Li, Q.M., Mines, R.A.W. and Birch, R.S. (2000). The Crush Behaviour of Rohacell-51WF Structural Foam, *International Journal of Solids and Structures*, **37**: 6321–6341.
3. Li, Q.M. and Mines, R.A.W. (2002). Strain Measures for Rigid Crushable Foam in Uniaxial Compression, *International Journal for Strain Measurement*, **38**(4): 132–140.
4. Koissin, V. and Shipsha, A. (2006). Deformation of Foam Cores in Uniaxial Compression-tension Cycle, *Journal Sandwich Structures and Materials*, **8**(5): 395–406.
5. Koissin, V. and Shipsha, A. (2001). Mechanical Properties of Pre-compressed and Undamaged Divinycell H-grade Foam Core, *Report C2001-5*, Dept. of Aeronautics, Royal Institute of Technology, Stockholm, Sweden.
6. Shipsha, A., Hallström, S. and Zenkert, D. (2003). Failure Mechanisms and Modelling of Impact Damage in Sandwich Beams—A 2D Approach: Part II—analysis and modelling, *Journal Sandwich Structures and Materials*, **5**(1): 33–52.
7. Rohacell (1987). Technical Manual, Röhm GmbH, Darmstadt.
8. Divinycell (1995). Technical Manual H-Grade, Divinycell Int. AB, Laholm.
9. Gibson, L.J. and Ashby M.F. (1988). Cellular Solids—Structure and Properties, Pergamon Press, Oxford.
10. Olsson, K.-A. and Lönnö, A. (1989). Test Procedure for Foam Core Materials. In: *Proc. of 1st Int. Conference on Sandwich Constructions*, pp. 293–318, Stockholm, Sweden.
11. Branner, K. (1995). Capacity and Lifetime of Foam Core Sandwich Structures, PhD thesis, Dept. of Naval Architecture & Offshore Engineering, Technical University of Denmark, Lyngby, Denmark.
12. Bull, P.H. (1998), Report S98-05, Dept. of Aeronautics, Royal Institute of Technology, Stockholm, Sweden.
13. Benderly, D., Zafran, J. and Putter, S. (2003). Shear Testing of Polymeric Foams, *Journal of Testing and Evaluation*, **31**(5): 405–412.